

Transcriptome and metabolome profiling of *Macrobrachium rosenbergii* reveals immune defense mechanisms against Decapod iridescent virus 1

Jing Chen, Xue-Mei Yuan, Meng-Yao Zhao, Jin-Biao Jiao, Lei Huang, Xian-Qi Peng, Jia-Yun Yao*

Zhejiang Institute of Freshwater Fisheries, Huzhou 313001, China

Introduction

Macrobrachium rosenbergii, commonly known as the giant freshwater prawn, belongs to the genus Macrobrachium.



After being infected with DIV1, the movement of *M. rosenbergii* slows down, its vitality sharply decreases, and a white triangular area called "white spot" appears on the basal shell of the rostrum. Some shrimp exhibit symptoms such as an empty midgut and atrophy of the hepatopancreas. Moreover, the virus has a fast transmission rate and a wide range of hosts, primarily outbreaks in the aquaculture areas of coastal provinces in China. Importantly, the virus detection and mortality rates in diseased shrimp are relatively high.

Like other crustaceans and invertebrates, shrimp lack an adaptive immune system and therefore rely on their innate immune system. Enhancing the survival and recovery of *M. rosenbergii* following DIV1 infection requires a thorough understanding of disease resistance related gene regulation, signaling pathways, and metabolic processes. In this study, we compared and observed virus particles in different tissues of *M. rosenbergii* infected with DIV1 using transmission electron microscopy. Furthermore, the artificial infection experiment was conducted to obtain the resistance and susceptibility individuals of *M. rosenbergii*. Integrating transcriptome and metabolome analysis, immune regulatory pathways and genes related to disease resistance were discovered. Therefore, this study provides important reference for understanding the molecular mechanisms of disease resistance in *M. rosenbergii* and aids in the breeding of new resistant varieties.

2. Morphology and Ultrastructure observation

We observed that the phenotype of *M. rosenbergii* appeared symptoms of redness from head to tail (Fig. 1A). Using TEM analysis, we detected the ultrastructure of *M. rosenbergii* tissues infected with DIV1, the result showed that the typical iridescent viral structures were presented in both hepatopancreas and gill tissues. Notably, a higher abundance of virions was observed in the gill tissue compared to the hepatopancreas (Fig. 1B).

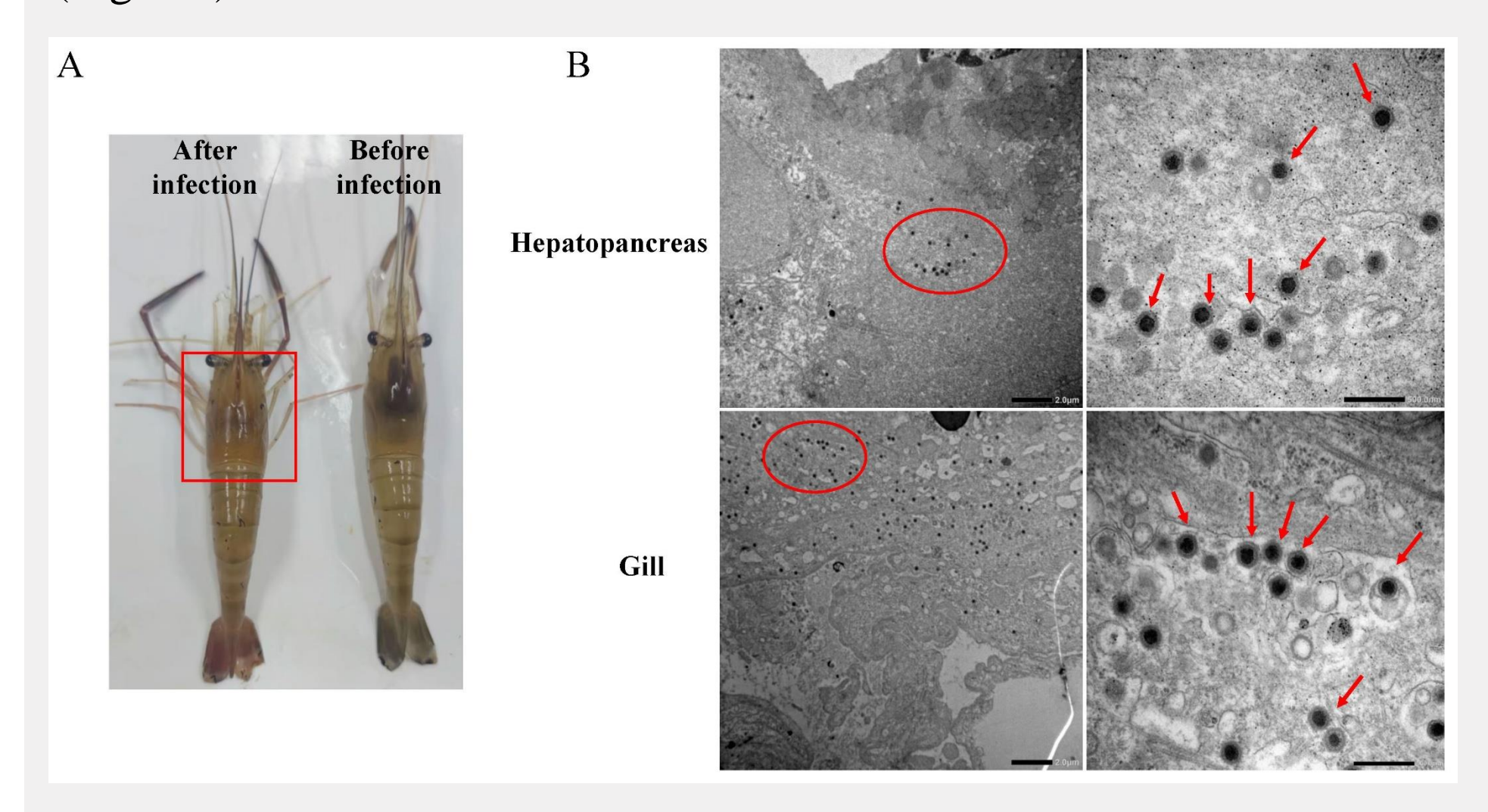


Fig. 1 The clinical signs (A) and transmission electron microscopy (TEM) visualization (B) of *M. rosenbergii* infected with DIV1.

RNA-seq profiling of *M. rosenbergii* infected with DIV1

The transcriptome profiles showed a high correlation with Pearson values ≥ 0.51 (Fig. 2A). Principal component analysis (PCA) indicated that the samples from control group (CK) and susceptible group (S) groups clustered together, suggesting similar expression profiles (Fig. 2B). The distribution of FPKM indicated a satisfactory level of data dispersion, suggesting good variability among samples (Fig. 2C). The clustering analysis showed that all three replicates of CK, resistant group (R), and S groups clustered together without obvious outliers, indicating good reproducibility (Fig. 2D).

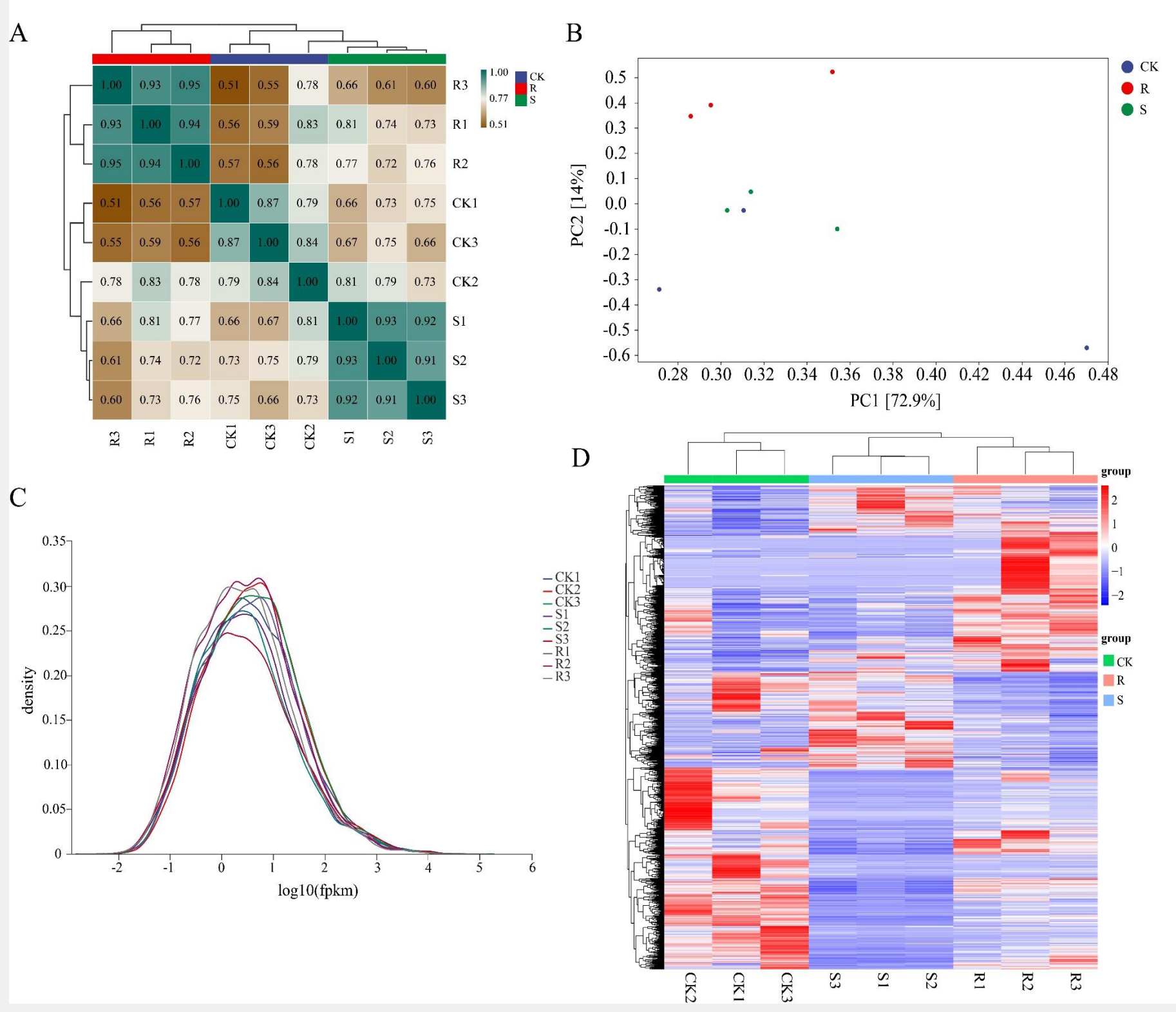


Fig. 2 RNA-seq profiling of DIV1 infected M. rosenbergii.

Differentially expressed genes (DEGs) and enrichment analyses

Through RNA-seq profiling analysis, a total of 4468 DEGs, encompassing both up- and down-regulated genes, were identified. Subsequent examination revealed that 863, 1131, and 708 up-regulated DEGs were identified for the CK-vs-R, S-vs-R, and CK-vs-S groups, respectively. The KEGG enrichment analysis after DIV1 infection revealed the enrichment of pathways such as oxidative phosphorylation, adipocytokine signaling, HIF-1 signaling, PI3K-Akt signaling, fatty acid biosynthesis, and ascorbate and aldarate metabolism (Fig. 3D).

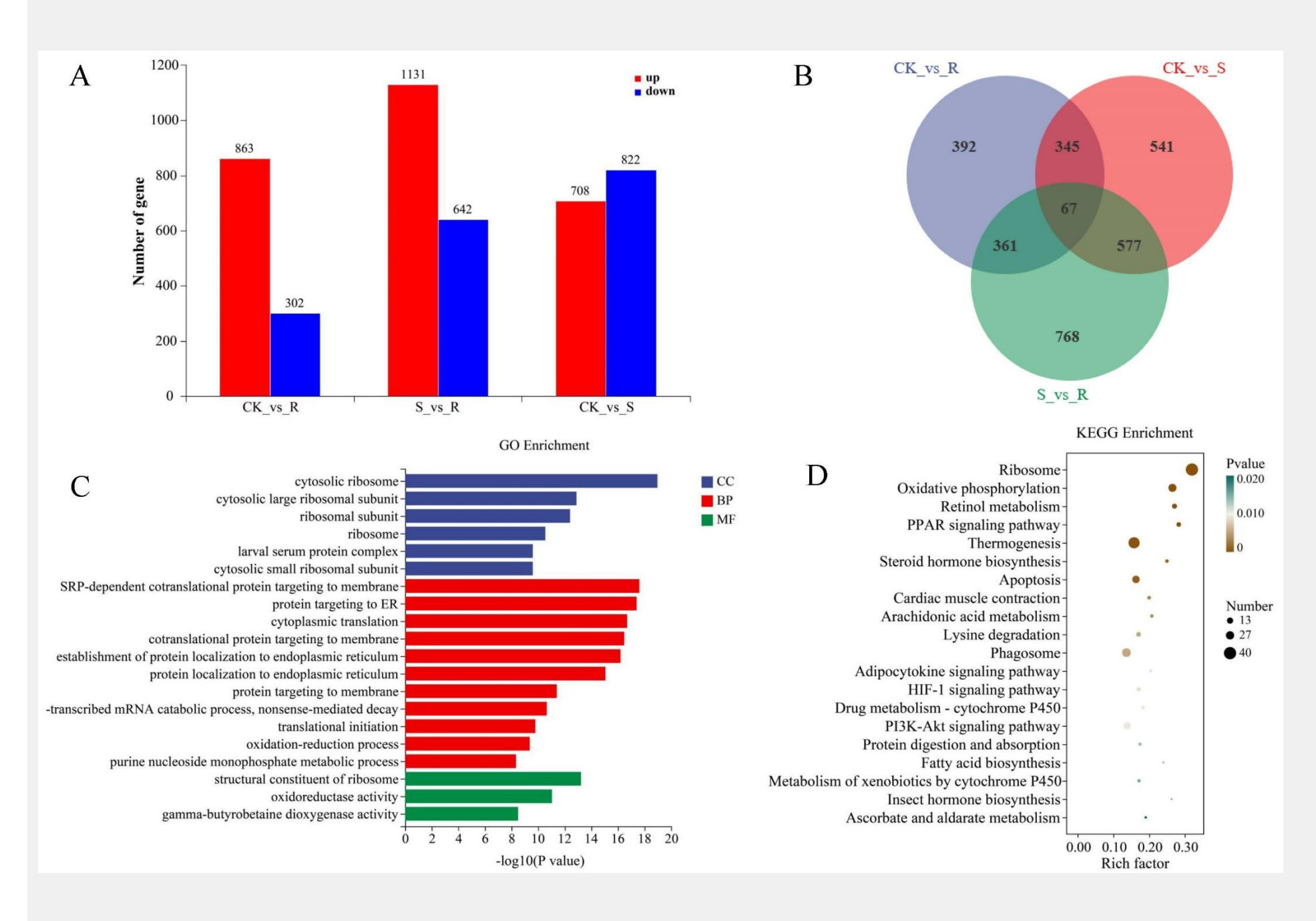


Fig. 3 Differentially expressed genes (DEGs) and enrichment analyses.

Metabolomic profiling of *M. rosenbergii* infected with DIV1

In the analysis of metabolomic profiling, 190, 224, and 80 down-regulated metabolites were observed in the S-vs-R, S-vs-CK, and R-vs-CK comparison groups, respectively (Fig. 4A). The result showed that the differential metabolites in S-vs-R were mainly enriched in pathways, such as biosynthesis of amino acids, ABC transporters, aminoacyl-tRNA biosynthesis, and protein digestion and absorption (Fig. 4B). Moreover, the network diagram revealed the significance of ABC transporters, biosynthesis of amino acids, aminoacyl-tRNA biosynthesis, and the regulation of lipolysis in adipocytes for metabolite synthesis or production (Fig. 4C). Notably, biosynthesis of amino acids, arginine biosynthesis, biosynthesis of various secondary metabolites part 3, and the mTOR signaling pathway were identified in the differential abundance score (Fig. 4D).

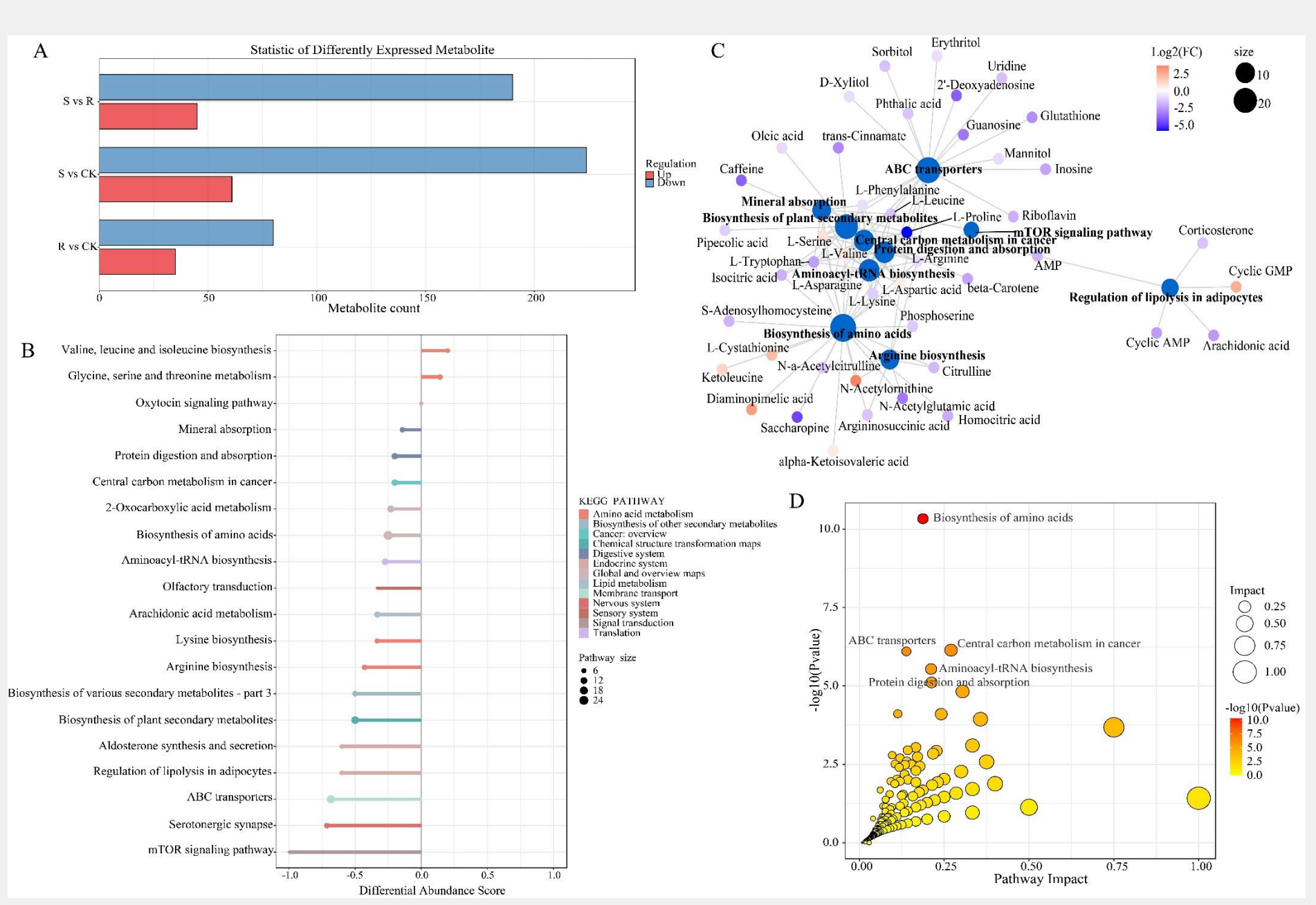


Fig. 4 The metabolomic profiling analysis of *M. rosenbergii* infected with DIV1.

Analysis of key metabolic pathway for M. rosenbergii infected with DIV1

The results indicated a significant association between amino acid levels and disease resistance, showing that the levels of N-a-Acetylcitrulline, Citrulline, and L-Arginine in the disease resistance group (R) were significantly higher than those in the control group (S) (Fig.5).

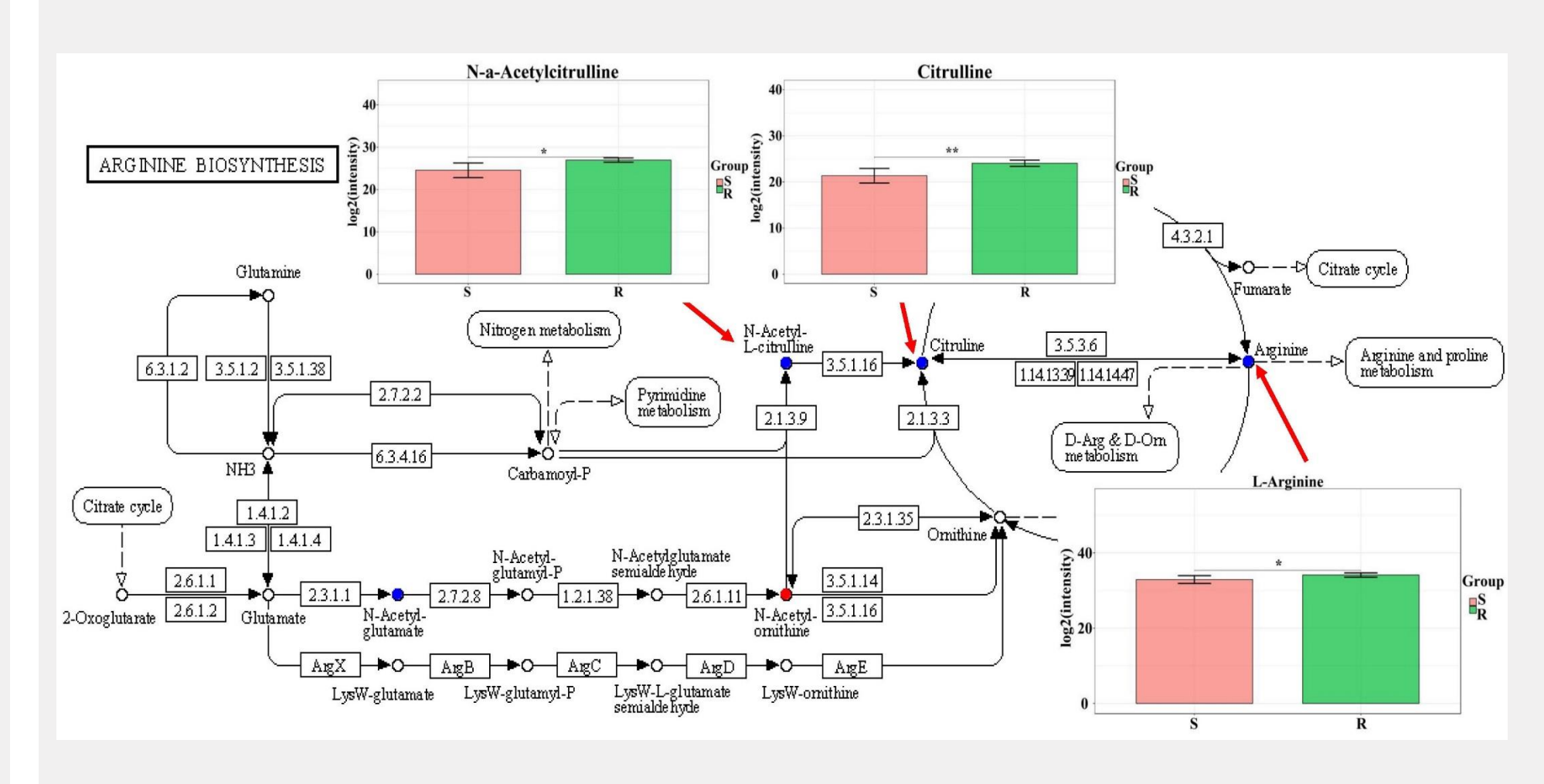


Fig. 5 The metabolic pathway analysis for differential metabolites in the arginine biosynthesis.

Integrated analysis of RNA-seq and metabolome profiling

Our observations indicate heightened expression of p38 in the MAPK signaling pathway in *M. rosenbergii* post-DIV1 infection. P38, a crucial signaling molecule in the MAPK cellular signaling pathway, actively engages in host cell processes during viral infection, regulating responses such as apoptosis and autophagy.

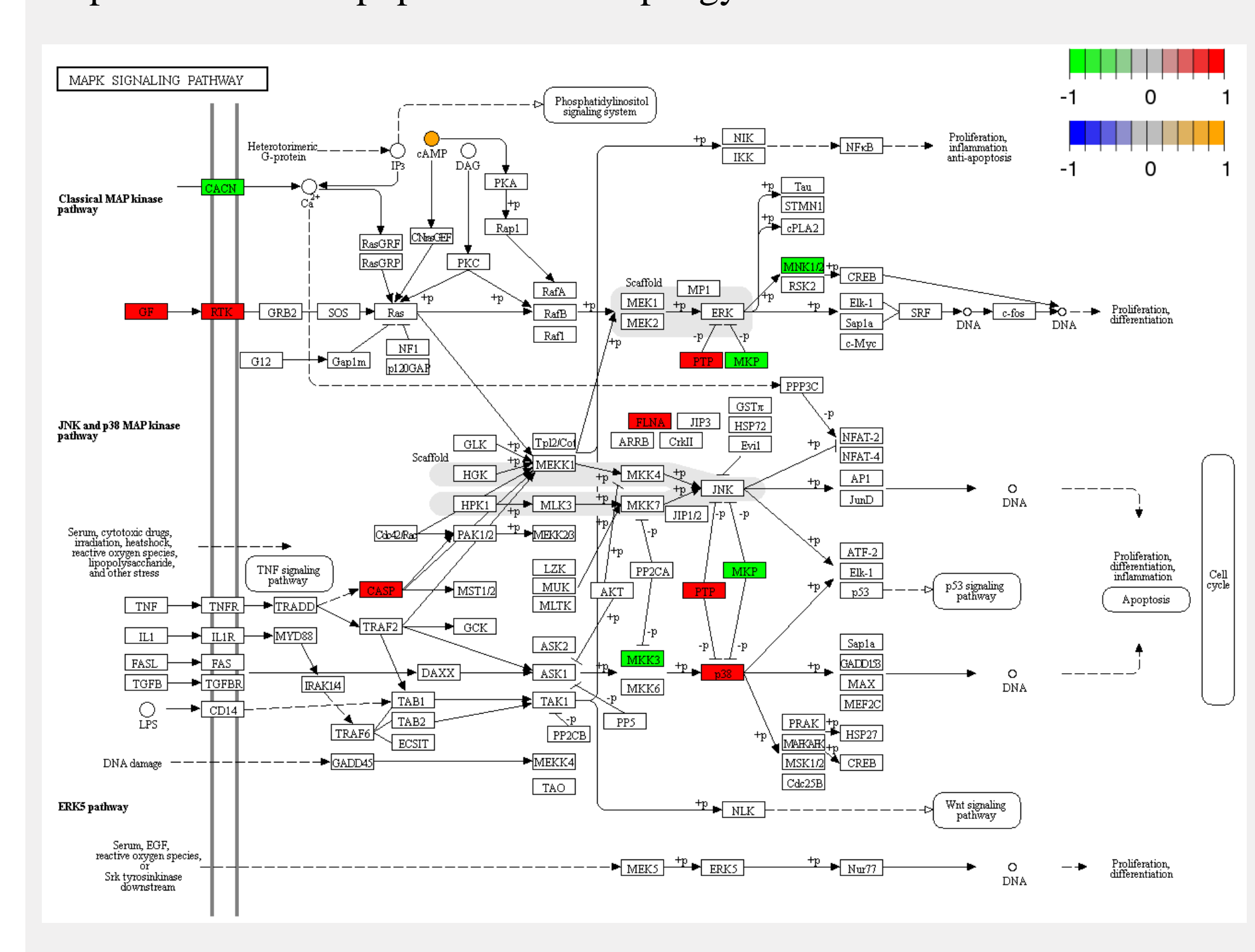


Fig. 6 The metabolic pathway analysis for differential metabolites and associated transcripts in the MAPK signaling pathway.

The result revealed a significant downregulation of CaV3 in the calcium signaling pathway. CaV3, belonging to low-voltage-activated calcium channels or T-type calcium channels, exhibits activation with relatively weak depolarizing stimuli and features low-voltage activation and rapid inactivation.

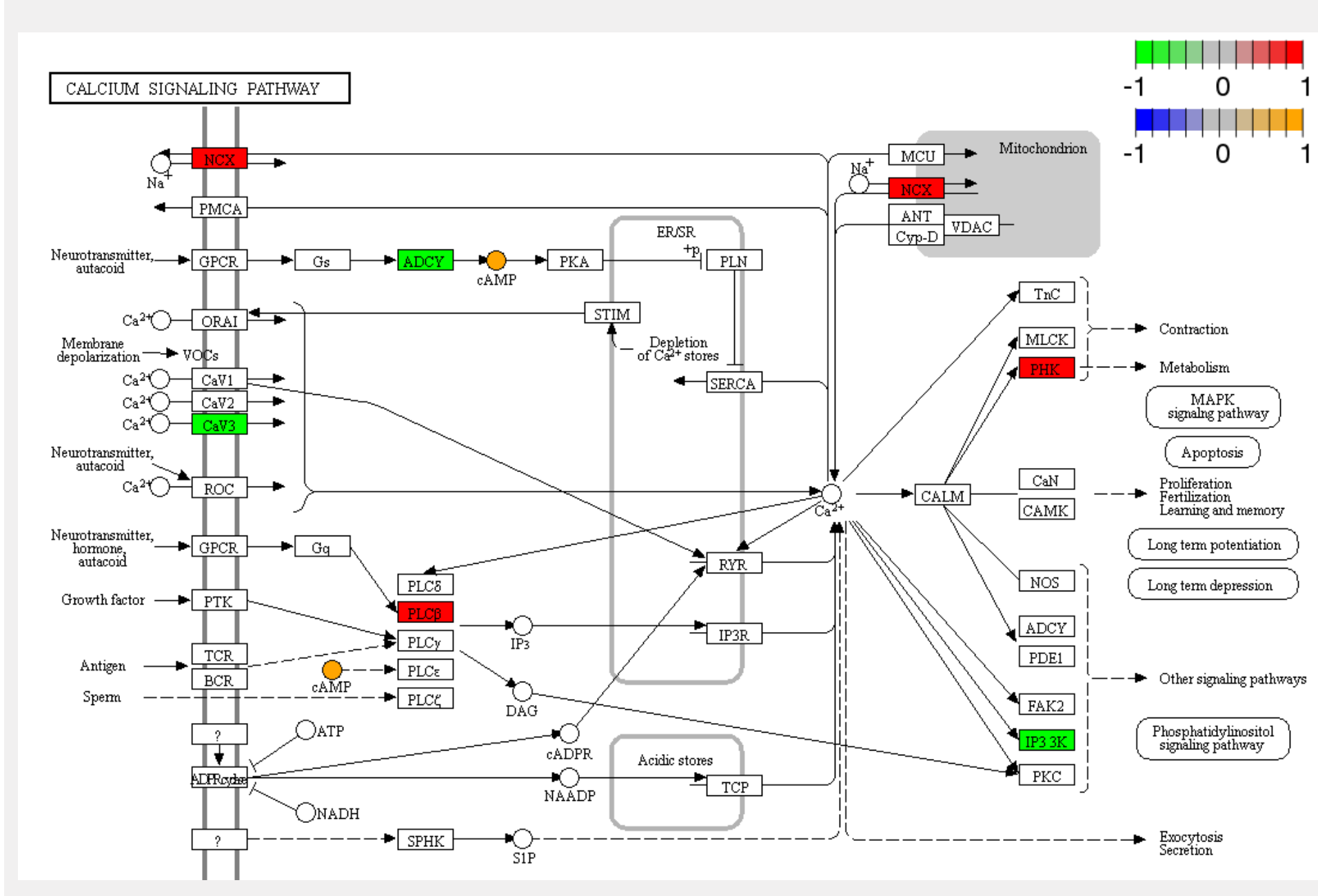


Fig. 7 The metabolic pathway analysis for differential metabolites and associated transcripts in the calcium signaling pathway.

8. Conclusions

In summary, this study revealed the immune defense mechanisms of M. rosenbergii during DIV1 infection, employing both metabolomic and RNA-seq analyses. Transmission electron microscopy uncovered characteristic iridescent viral structures in both hepatopancreas and gill tissues. RNA-seq analysis revealed that oxidative phosphorylation, adipocytokine signaling, HIF-1 signaling, PI3K-Akt signaling, fatty acid biosynthesis, and ascorbate and aldarate metabolism were enriched post DIV1 infection. In the metabolomic profiling analysis, pathways such as biosynthesis of amino acids, arginine biosynthesis, biosynthesis of various secondary metabolites part 3, ABC transporters, and the mTOR signaling pathway were identified. Through integrated analysis of metabolomic and RNA-seq data, p38 in the MAPK signaling pathway and CaV3 in the calcium signaling pathway emerged as potential key players in conferring resistance to DIV1 virus invasion. These findings hold promise for advancing disease prevention and RNAi vaccine development for *M. rosenbergii*.

9. Funding

This work was supported by the Zhejiang Key Research and Development Project (No. 2024C02005 and 2022C02027), the Key Research and Development Project Program of Huzhou City (No. 2023ZD2032), and the Zhejiang Provincial Institute Special Project (No. 2024YSZX01 and 2024YSZX04).